

DD

# GSI

GSI-Preprint-95-74  
NOVEMBER 1995

## PESTOV SPARK COUNTER PROTOTYPE DEVELOPMENT FOR THE CERN-LHC ALICE EXPERIMENT

E. BADURA, J. ESCHKE, H. GAISER, H.H. GUTBROD, U. KOPF, Ch. NEYER,  
B. ROTERS, H.R. SCHMIDT, R. SCHULZE, P. STEINHAUSER, H. STELZER,  
A.R. FROLOV, Yu.N. PESTOV, M.A. TIUNOV, V. DODOKHOV

SCAN-9601263



CERN LIBRARIES, GENEVA

sw 95 06

Gesellschaft für Schwerionenforschung mbH  
Postfach 1105 52 · D-64220 Darmstadt · Germany

# **Pestov Spark Counter Prototype Development for the CERN-LHC ALICE Experiment**

E. Badura, J. Eschke, H. Gaiser, H.H. Gutbrod<sup>\$</sup>, U. Kopf, Ch. Neyer,  
B. Roters<sup>†</sup>, H.R. Schmidt, R. Schulze, P. Steinhäuser\*, H. Stelzer  
*GSI Darmstadt*

A.R. Frolov, Yu. N. Pestov, M.A. Tiunov  
*BINP Novosibirsk*

V. Dodokhov  
*JINR Dubna*

A prototype Pestov Spark Counter with 2-dimensional position resolution has been developed. The position resolution is 0.32 mm and <2mm in transverse and longitudinal direction, respectively. Beam tests yielded both the time resolution and the efficiency in accordance with earlier results obtained at BINP Novosibirsk. A longterm stability test has been performed and stable behaviour for more than 3 months was observed.

## **I. Introduction**

Future RHIC and LHC heavy-ion experiments envision mid-rapidity TOF measurements with detector areas of up to 150 square meters. The number of charged particles per unit rapidity,  $dN_{\text{Ch}}/dy$  is expected to be up to 8000 for Pb+Pb collisions at the LHC. In order to cope with these many particles, detector systems must have a large number of cells (in order to avoid double hits) at a "reasonable" price-per-cell. Conventional TOF systems, i.e., scintillators with photomultiplier readout, are known for their good performance characteristics. They suffer, however, from a relatively high price, mainly due to the cost for high resolution photomultipliers.

The use of parallel-plate spark counters (Pestov Counters) offers a possibility of high time (up to 25 ps) and position resolution (300-500  $\mu\text{m}$ ) [2-7]. The detection efficiency is close to 100%, and the counting rate capability is by far sufficient for typical heavy-ion experiments.

---

<sup>\$</sup> present address: CERN, PPE-Division, CH-1211 Geneva 23

<sup>†</sup> present address: 1024, Key Route Blvd., Albany, CA 94706, USA

\* present address: University of Karlsruhe, 76021 Karlsruhe

An, -in principle -, relative simple construction and a high intrinsic gain makes this type of counter a promising candidate for large scale applications, where high resolution at a low per-channel price is required.

In this paper we shall describe the construction and subsequent tests of Pestov Spark Counters as prototype development for the ALICE<sup>1</sup>[1] experiment. The objective of the project is to develop means of mass production of this type of counter in order to allow its application in large scale experiments. The design of the counter presented in this article has already many features, - although of a prototype level -, which are envisioned for a large ALICE TOF barrel.

In Section II we shall give the technical details of the design of the counter, while in Section III the result of a test employing a particle beam as well as a long term stability test with a  $\gamma$ -source shall be discussed.

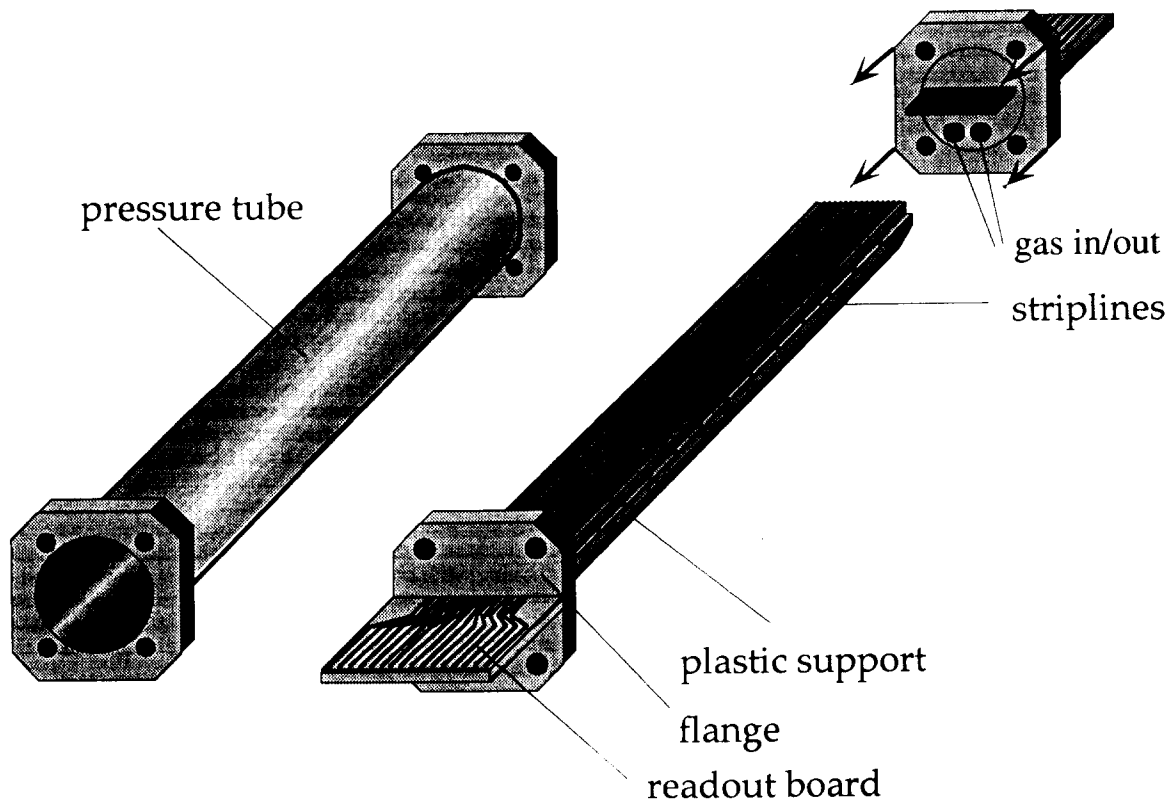


Fig. 1 Artists view of the Pestov Spark Counter. Shown on the left is the pressure container. The right side shows the assembled counter together with the readout boards glued into the flanges at both ends.

### 1.1. Working Principle

The Pestov Spark Counter [2-7] is a single-gap, gaseous parallel-plate detector working in the streamer/spark mode. It features the use of a semi-conductive anode and of a special gas mixture that keeps the discharge local and enables a high global counting rate capability. The time resolution improves with decreasing gap size. For the ALICE TOF application a gap

<sup>1</sup> ALICE,- A Large Ion Collider Experiment-, a dedicated heavy-ion experiment at the CERN LHC.

between the electrodes of  $100\ \mu\text{m}$  was chosen as a compromise between amplitude height, necessary for the front-end readout electronics, and the desired time resolution. The counter operates at a pressure of  $\approx 12\ \text{bar}$ , which yields 4-5 primary electrons from a minimum ionizing particle. A voltage of up to  $6\ \text{kV}$  is applied to the electrodes. The spark, initiated in the gap after the passage of a charged particle, discharges only a limited area of the semi-conductive anode ( $\approx 1\text{-}2\ \text{mm}^2$ ), while the remaining area of the anode remains sensitive to other charged particles.

The version of the Pestov Spark Counter described in the article has been proposed by Yu. Pestov and built recently in collaboration with GSI. It has the essential new feature that it is read out via 16 finely spaced ( $2.54\ \text{mm}$  pitch) conductive strips placed on the back side of the anode. The readout through stripline allows the two-dimensional reconstruction of the location of a spark. The longitudinal position is deduced from the time-difference of the signal arrival time at the two ends of the strip while the transverse position is obtained from the weighted mean charge over several excited strips. From a mechanical point of view the radiation length of the detector is reduced by using a cylindrical pressure tube. For this layout a new support structure and gas distribution inside the counter have been developed.

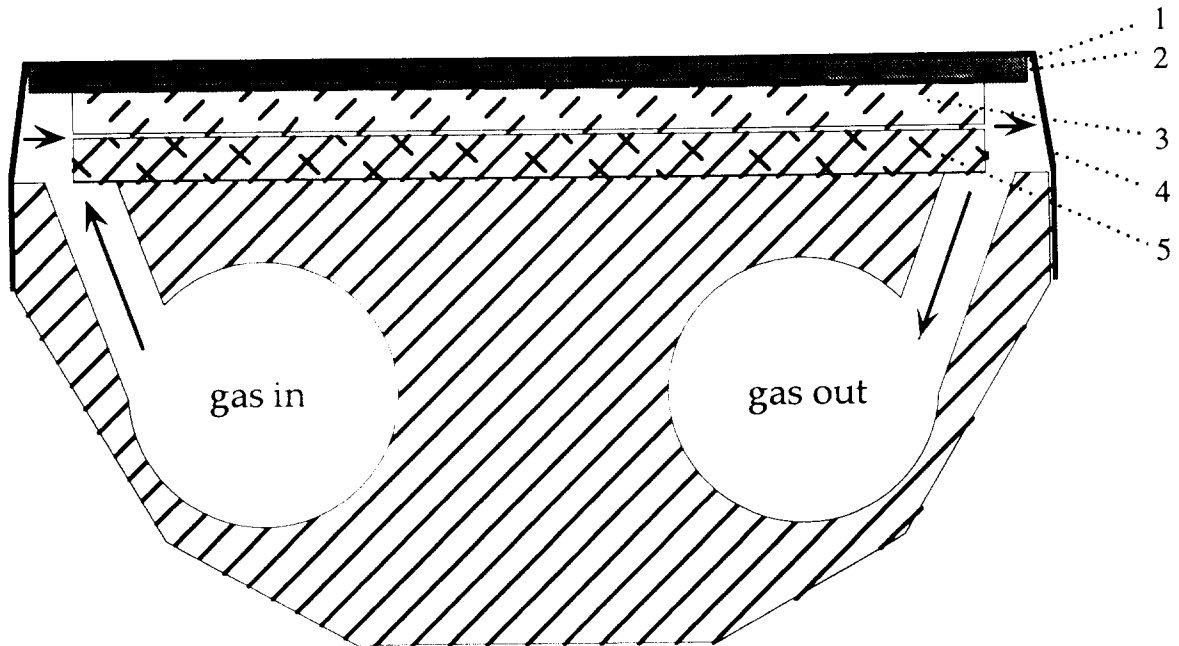


Fig. 2 Cross section of the counter at the location of a gas connection to the gap between the electrodes. (1) FR4 cover plate; (2) readout strips; (3) anode; (4) gas seal; (5) cathode.

## II. Construction Details and Assembly

A schematic, 3-dimensional view of the counter is depicted in Fig. 1. The active size of the counter, i.e., the dimension of the electrodes, is  $40.68 \times 540.8\ \text{mm}^2$ . The backside of the semi-conductive electrode has 16 gold readout strips evaporated onto. The width and pitch of the strips are  $1.27\ \text{mm}$  and  $2.54\ \text{mm}$ , respectively. The striplines are connected at each end to a

multilayer board. Each multilayer board has itself 16 short striplines, which are coupled to the strips on the glass via thin gold plated springs. The multilayer boards are glued into the flanges which close the pressure vessel. The two electrodes are mounted onto a plastic support structure shown in a cross section view in Fig. 2. The support structure for the electrodes also forms the gas channels. To maintain a gas flow through the gap between the electrodes a pressure difference between the left and right gas channel is applied by a circulation pump. The gas channel is coupled via a series of small holes to the sealed space directly left and right of the gap, from where the gas is forced to flow through the gap between the electrodes. The pressure tube around the counter is made of 1 mm thick aluminum and has an outer diameter of 50 mm.

The three plates, i.e. the cathode, the semi-conductive glass and the FR4 plate (omitted in Fig.1) form, together with the strips on the glass and the FR4 plate a  $50 \Omega$  wave guide: the ground plane on the FR4 plate and the HV cathode are the boundaries, while the semi-conductive glass ( $\epsilon=8$ ) and the FR4 plate ( $\epsilon=4$ ) serve as dielectric around the strip lines.

The "critical" elements concerned here for the construction and assembly of a Pestov Spark Counter are a) the spacers to maintain the spark gap of  $100 \pm 2.5 \mu\text{m}$  at a field of up to  $0.6 \text{ MV/cm}$ , and b) the surface quality of both cathode and anode. Furthermore, it is important to maintain clean room conditions during assembly and not to expose the electrodes to any source of dust or dirt during operation.

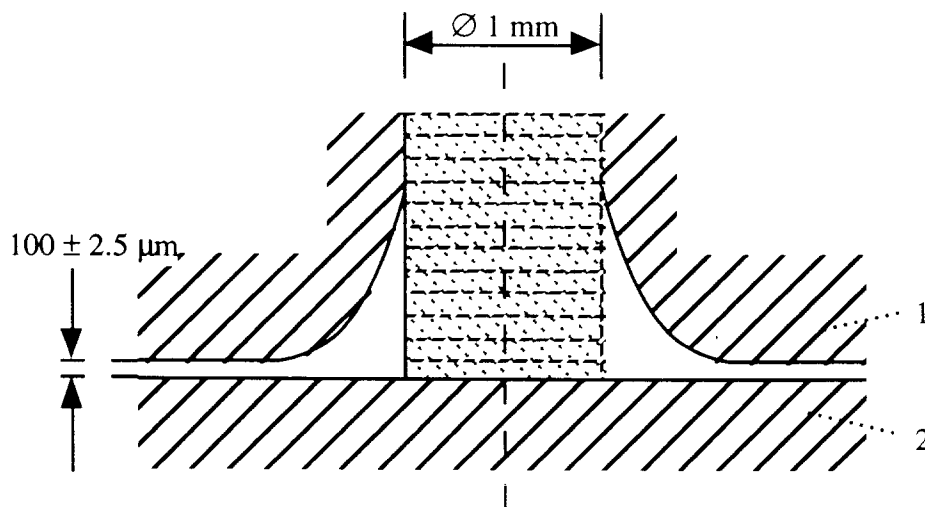


Fig. 3 Cross section through a spacer. The spacer is glued into a hollow and adjusted to keep the distance between the electrodes within  $100 \pm 2.5 \mu\text{m}$ . (1) semi-conductive electrode; (2) cathode.

## II.1. Spacers

To avoid break-down of the electric field at the spacers it is decreased sufficiently by changing the distance between cathode and anode locally, i.e. by drilling hollows as indicated in Fig. 3. These hollows house the spacers, which are cylindrical glass pins glued into holes

drilled through the semi-conductive glass and adjusted individually to the right length of 100  $\mu\text{m}$  with a special tool. The edges of the hollows (as well as the edges of the plate) were rounded carefully to keep the increase of the field here at a minimum [8]. A grid ( $d=22\text{ mm}$ ) of spacers is manufactured into the semi-conductive anode in order to keep the sagitta due to the electrostatic pressure ( $6.4\text{ N/cm}^2$ ) below  $\approx 0.2\%$  of the gap distance.

## II.2. Coating

For this prototype the cathode used was made of standard 2 mm float glass coated via vacuum evaporation by Cr-Cu-Cr-Cu being 200, 2000, 200 and 5000  $\text{\AA}$  thick, respectively. After evaporation of the first copper layer the electrode was cleaned in order to remove metal-covered dust grains. The resulting pin holes on the surface were eliminated by the evaporation of a second layer. It turned out that direct evaporation always led to a small number of copper pins that were splashed onto the surface presumably by "micro explosions" in heated the copper container. This could be remedied by using diffusion evaporation, i.e. shielding the cathode from the direct exposure by the copper beam.

It should, however, be noted that for the tests described below cathodes from direct evaporation were used.

## II.3. Cleaning

The entire assembly of the counter was done under clean room conditions in a laminar flow module. Before the assembly the electrodes were cleaned thoroughly. The surfaces were first mechanically cleaned with cerium oxide powder and then rinsed with triple distilled water. To avoid any touching of the electrodes front sides vacuum supports were used. During the whole washing procedure the electrode surfaces were kept facing down, i.e. in the direction of the air flow thus avoiding exposure to remaining dust particles.

# III. Detector Tests

## III.1. Discriminator

The pulse risetime of signals from Pestov Spark Counters is known [2] to be less than 300 ps. Therefore, it is expected that standard leading edge discriminators, which are usually not optimized to high frequencies will limit the overall time resolution. Several leading edge discriminators were tested to obtain their response to fast pulses and in particular the time delay of the output as function of the amplitude of the input signal ("walk"). The results are shown in Fig. 4. Both the LeCroy 623 and the GSI 8001 discriminators exhibit a similar walk curve. For these characteristics amplitude fluctuations of  $\Delta A/A \approx 0.5$  would result in an electronic contribution to the time resolution of  $\sigma \approx 70\text{ ps}$ . Amplitude fluctuations of this magnitude are conceivable resulting both from intrinsic fluctuations of the discharge itself as

well as from geometric fluctuations. The latter ones come from variation of the location of a spark with respect to the pickup strip. Finally, it should be remarked that the constant fraction technique for walk correction cannot be used for hardware walk correction because of the varying shape of the pulses. Also slewing corrections, done usually for scintillator counters, are, for the same reason, not very efficient. The measurement of the time relies entirely on the fast risetime of the particle-induced spark since, due to secondary discharges the trailing part of the pulse varies strongly in shape.

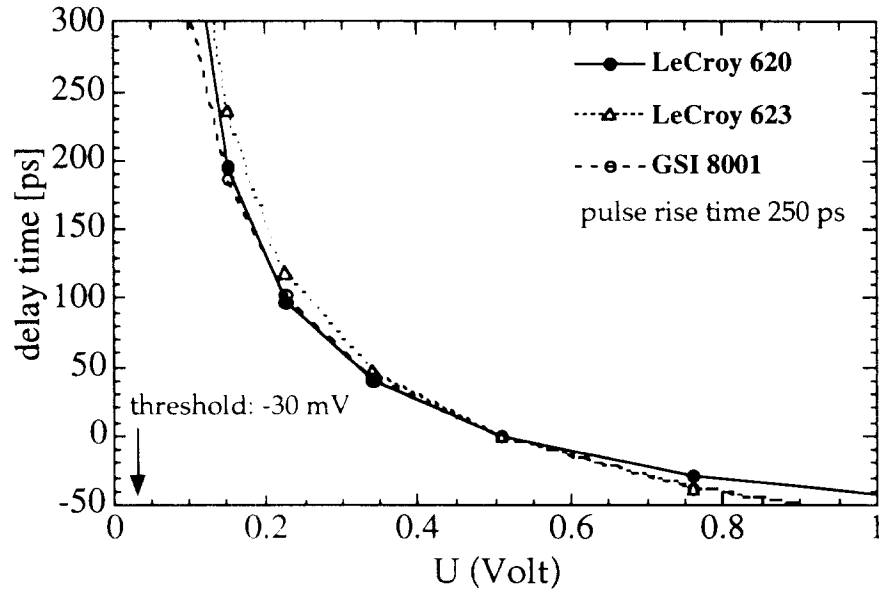


Fig. 4 Delay of the discriminator output signal for different input pulse height ("walk"). The rise time of the input pulse was 250 ps; the threshold was set to -30 mV.

It should, however, be remarked that presently a novel type of discriminator [9] is being developed at Novosibirsk and at GSI which, as first test have shown, should be able to measure  $t_0$  of pulse of varying height with a precision of better than 6 ps ( $\sigma$ ), thus giving hope that the above problems shall be solved in the near future.

### III.2. Counter Performance in a Test Beam

Two counters of the type described above were tested in a secondary beam at the CERN SPS. The two counters were mounted directly behind each other. Two scintillator slabs installed in front and behind of the two Pestov counters, respectively, were used for triggering. The particles in the beam were mostly minimum ionizing pions; no effort was taken to discriminate against electrons or protons. The beam was defocused to about 3 cm to illuminate a large part of the detectors. Simultaneously, the detectors were exposed to a strong  $^{60}\text{Co}$   $\gamma$ -source leading to a counting rate of about 2 kHz with no beam. The main purpose of the  $\gamma$ -source was to initiate sufficient discharges for the so-called "burning-in" [2]. A gas flow through a counter of about then 10 l/min, corresponding to a gas velocity in the spark gap of

$\approx 3$  m/s was maintained. As gas the "standard" mixture [2] consisting of 76.9% argon, 20.0% isobutane, 2.5% ethylene and 0.6% divinyl at a pressure of 12 bars was used.

Each of the 64 channels (2 x 16 striplines read out at both ends) was connected with a short cable to a GSI 8001 leading edge discriminator. From there, standard NIM pulses were sent to the TDC's. The trigger signal for the DAQ was provided by a coincidence of the two scintillator counters. The amplitude signal of each strip was taken from an emitter follower circuit in the GSI8001 discriminators and fed to LeCroy 2228 charge integrating 11-bit ADC's with a sensitivity of 0.5 pCb/channel.

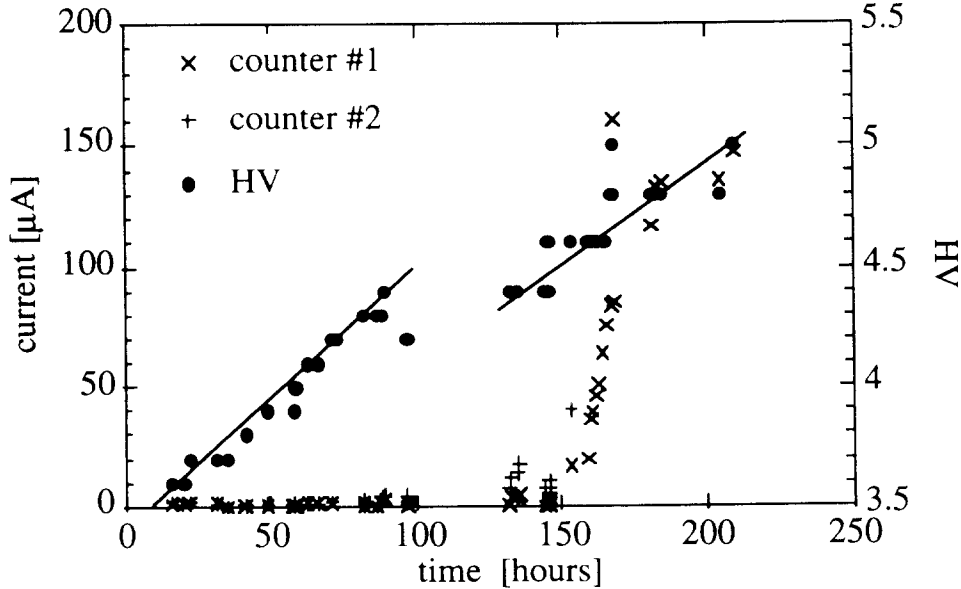


Fig. 5 Left axis: current drawn by the two counters as a function of time during the run. Right axis: high voltage applied to the counters.

During the first 150 hours of test beam the high voltage was raised linearly with time from the threshold voltage of 3000 V to 4400 voltage. During this period the background counting rate, -monitored by measuring the "dark" current drawn by the counter was on a low level ( $< 2$  Hz/cm<sup>2</sup>). The corresponding current, shown in Fig. 5 as function of time, is below 0.5  $\mu$ Amp. At voltages close to 4.4 kV a small increase of the current could be observed which is explainable by some increase in the background counting rate due to the onset of auto-electron emission at surface defects, i.e. the accidental copper pins or splashes on the cathode produced during evaporation. A sudden and large increase of the current to a level  $> 100$   $\mu$ Amp corresponding to 14 kHz global background counting rate was observed in both counters after 175 hours of operation.

These effects, i.e. background occurring at pins and a drastic increase in background rate will be discussed in detail in the next section, where we present the results of a dedicated investigation of the long term stability. In this section we shall focus on the time and position resolution and efficiency obtained with beam particles. It should be mentioned that in a triggered mode no influence or deterioration on the data taken by the background was noticed.



### III.2.1 Position Determination and Resolution

The counter provides position resolution in two dimensions. The position of a discharge in strip direction, i.e., longitudinal, is limited by the resolution of the electronics, and here mainly by the binning of the time digitizer. The walk of the discriminator is of less importance, since the signals seen at two ends of a strip come from the same spark and do not fluctuate against each other. Given the binning of 50 ps of the TDC used and a signal velocity of 14 cm/ns a simple estimate yields  $\sigma \approx 2$  mm as lower limit of the resolution in strip direction. This estimate is verified by the experimental result as shown in Fig. 6, where  $\sigma \approx 2$  mm longitudinal position resolution was measured.

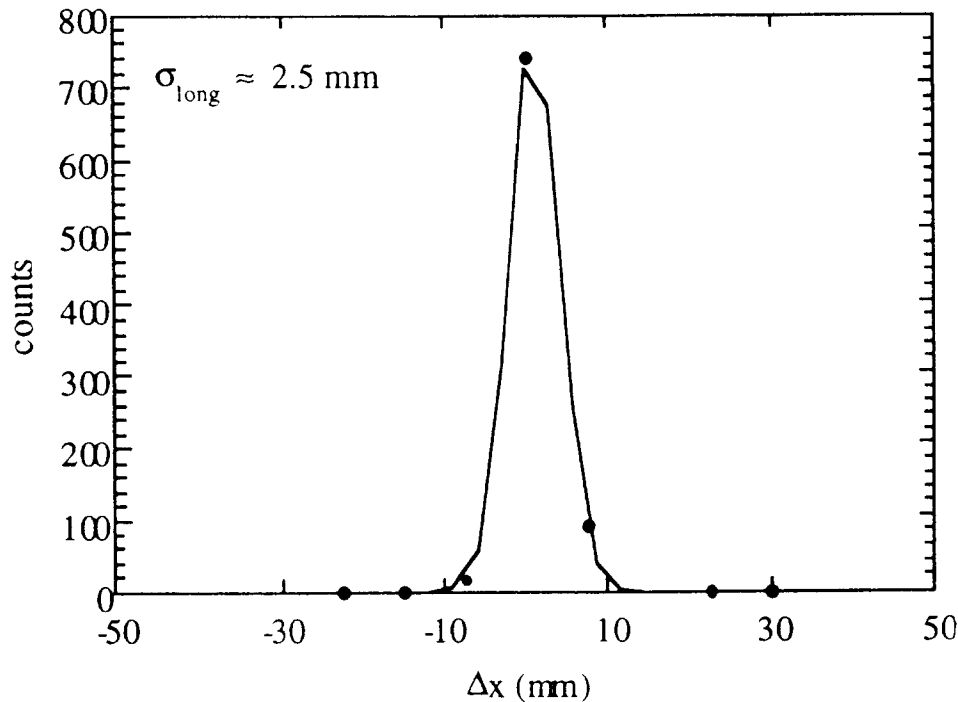


Fig. 6 Longitudinal position resolution of the counter obtained from the time difference of the signal arrival time.

The transverse position resolution is based on the fact that a point like discharge will, due to the 2 mm thickness of the anode, induce a signal on the backside strips over an area with roughly this diameter. Given a distance of 2.54 mm between the centers of two adjacent strip it is evident that, in the average 2-3 strips should "see" a spark. The experimentally measured strip multiplicity per spark is shown in Fig. 7. This characteristics allows to find the spark position by the center of gravity method with high precision. The average position resolution obtained from the comparison of the spark location in the two spark counters is shown in Fig. 8 and turns out to be  $\sigma \approx 320 \mu\text{m}$ .

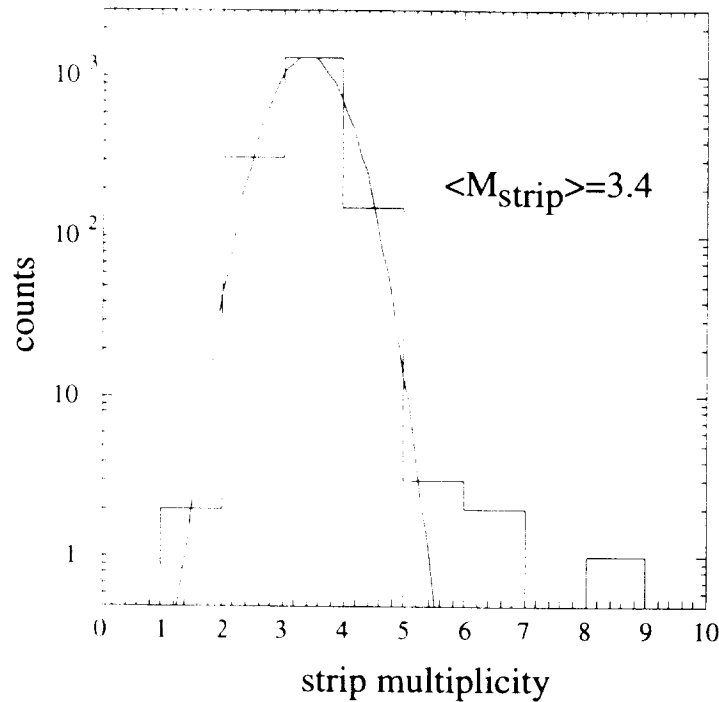


Fig. 7 Average multiplicity of strips excited after a charged particle initiated a spark in the gap between the electrodes.

### III.2.2 Efficiency

The efficiency of particle detection of the Pestov spark counter was measured by comparing the counting rate in the two counters when exposed to a particle beam, where one of the counters is used as "trigger" counter. To avoid particle loss due to misalignment of the two counters a sufficiently small area in one Pestov counter was (offline-) selected such that full overlap of this area with the other spark counter was guaranteed. The experimentally measured efficiency at 4.4 kV is 94%. This result is in agreement with result obtained at Novosibirsk [10].

### III.2.3 Time resolution

In order to minimize pulse height fluctuation, which, for the reasons discussed above, would mask the intrinsic resolution of the counter by electronic effects, several cuts were applied to the data: i) the location of the sparks was selected to be directly underneath a strip thus reducing the fluctuation induced by geometry; ii) a certain reduction of the fluctuations inherent to the discharge process itself is obtained by selecting sparks with high integrated charge.

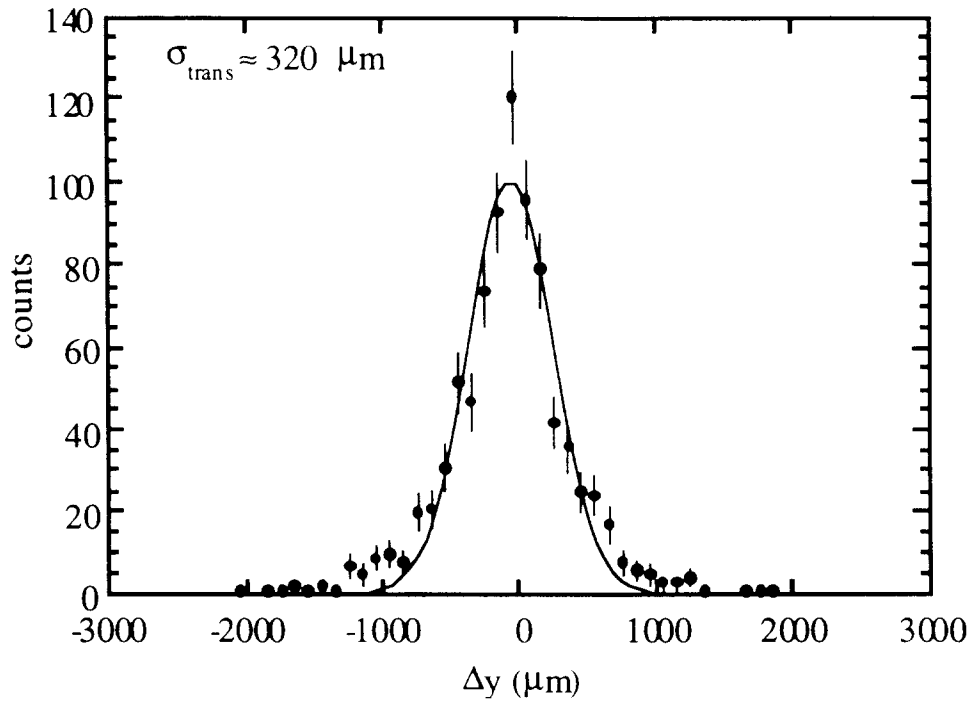


Fig. 8 Transverse position resolution of the counter obtained from the weighted mean over several strips.

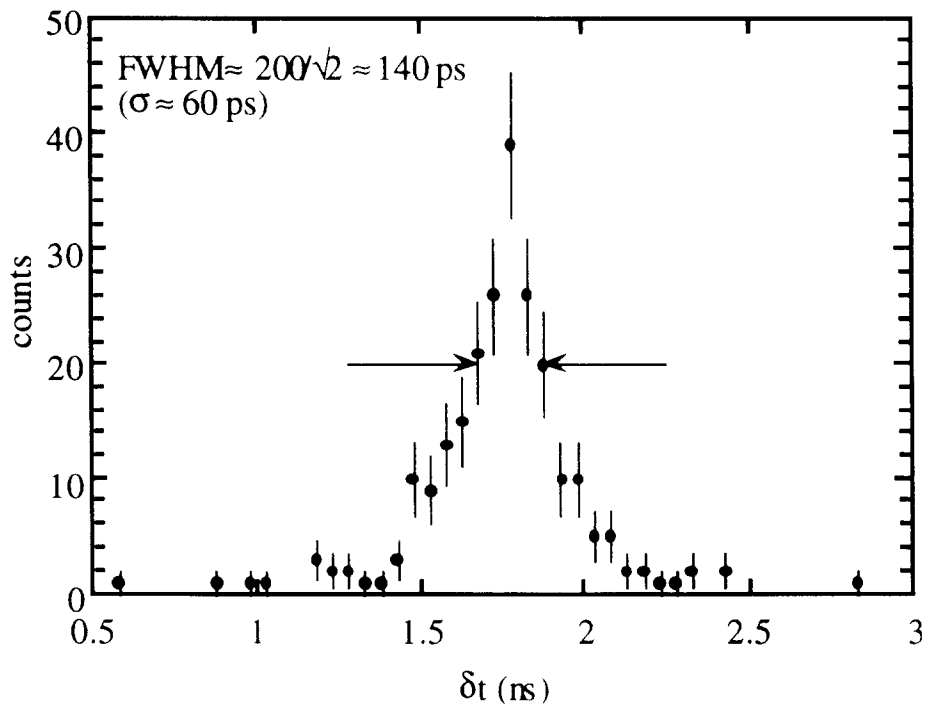


Fig. 9 Intrinsic time resolution of the counter obtained from the time difference measured between two identical counters.

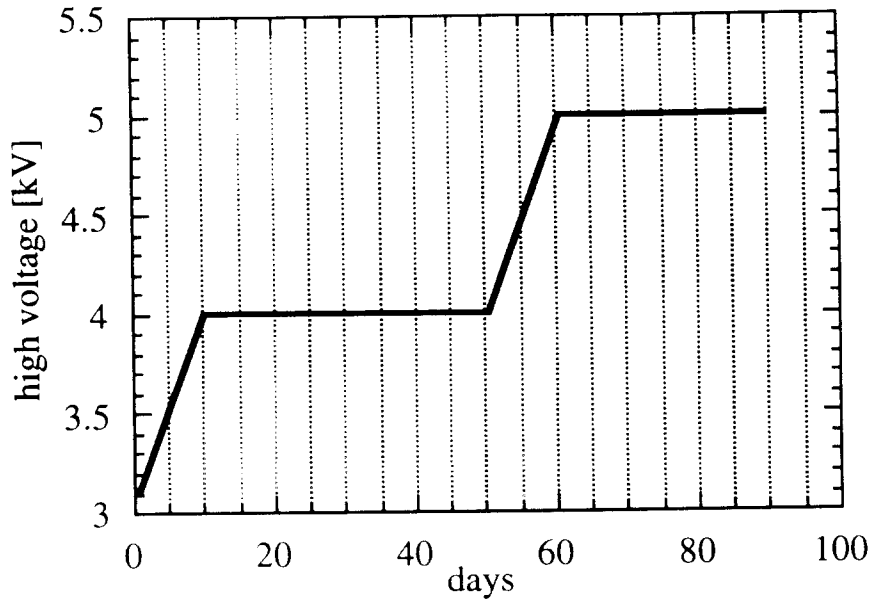


Fig. 10 High voltage applied to the counter during the long term stability test as a function of time

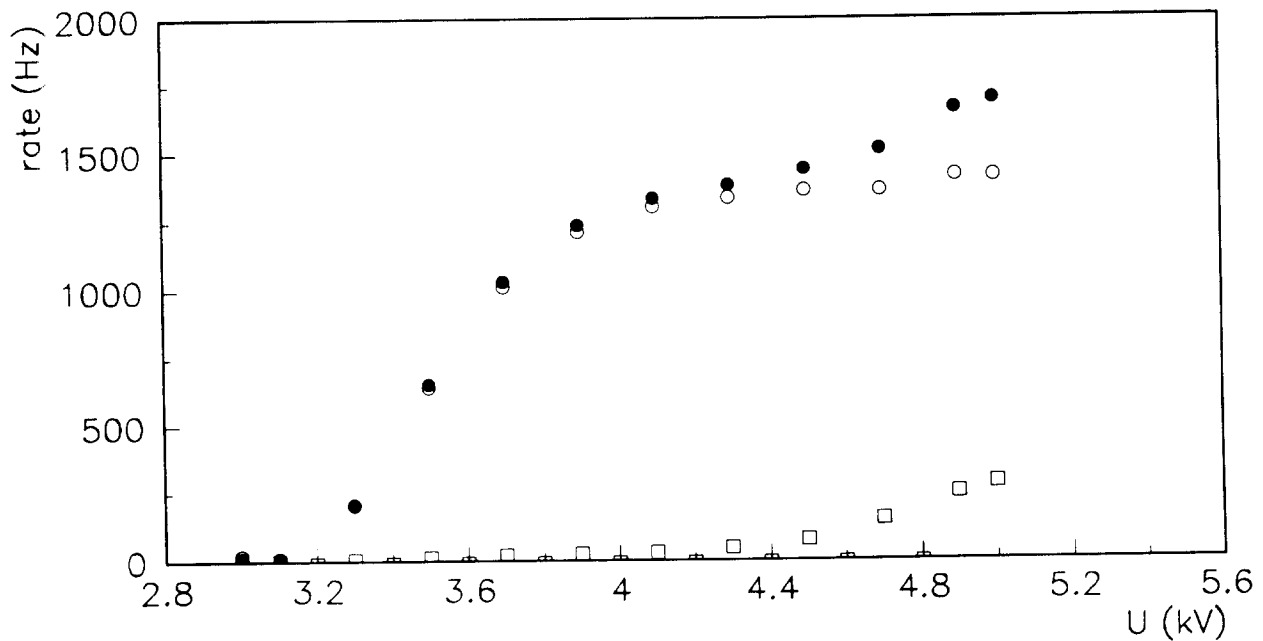


Fig. 11 Rate from a  $\gamma$ -source (closed circles) vs high voltage applied to the counter ('plateau curve'). The open squares show the background counts obtained without source. The open circles show the plateau curve with the background rate subtracted.

Even though the second cut is not very efficiently selecting pulses of similar amplitude (because of afterpulses due to secondary sparks destroying the correlation between amplitude and integrated charge) the time resolution measured at 4.4 kV is  $\text{FWHM} \approx 140 \text{ ps}$  ( $\sigma \approx 60 \text{ ps}$ ) (Fig. 8). This corresponds to the value expected for the intrinsic resolution from earlier measurements at Novosibirsk [1,2].

### III.3. Long Term Stability Test

Previous measurements of the long term behavior had been carried out over period of about 20 days. It was the aim of the present experiment to extend the time range significantly. With the cathode used both the stability in "good" areas, i.e. no surface defects, as well as under extreme conditions at the location of copper pins could be investigated.

Fig. 10 displays the voltages applied to the counter over the test period of  $\approx 90$  days. The HV was raised slowly over a period of one week from the threshold of 3 kV to the onset of the plateau at 4 kV. There it was kept constant for about 1 month and then increased to 5 kV. At 4 kV and below the counter was permanently exposed to a strong  $\gamma$ -source for 'burning-in'. At 5 kV the source was removed. It should be noted that the gas flow through the counter has been decreased by a factor of 3 as compared to beam test.

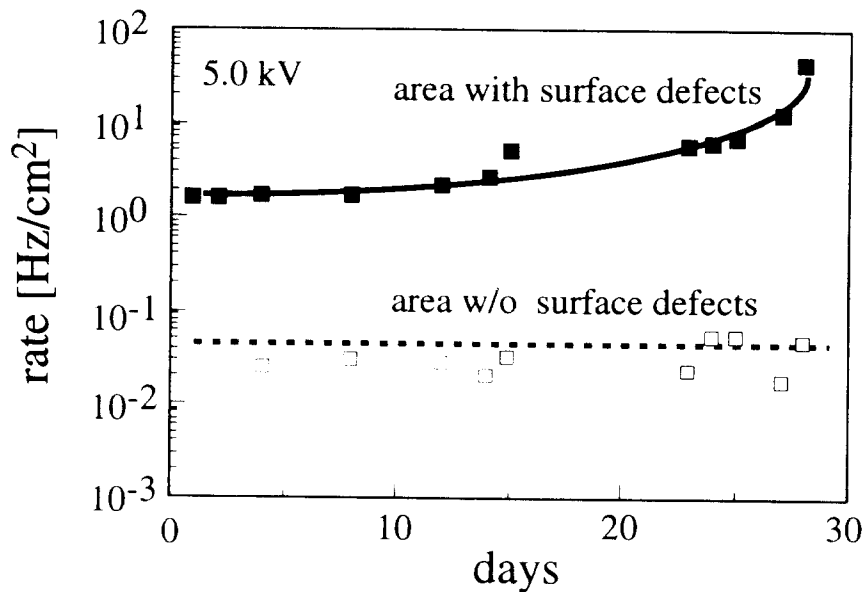


Fig. 12 Background rate of the counter at 5 kV. The open squares show the counting rate, where areas with surface defects were excluded. The black squares give the overall counting rate. The lines are to guide the eye.

Figure 11 shows the plateau curve of the counter. The full circles indicate the counting rate with  $\gamma$ -source irradiation. The 'squares' show the rate of the counter without source as a function of voltage. A slight increase of background discharges set on at 4.3 kV. After subtraction of these background discharges a saturation of the rate, i.e. a plateau, beginning from 4 kV can be seen (open circles).

Fig. 12 shows the background rate at 5 kV over a period of 1 month. The background rate slowly increased with time from 0.3 to 1 kHz and then suddenly to 8 kHz. Due to the 2-dimensional position resolution the spatial distribution of background discharges can be reconstructed and is shown in Fig. 13a at the beginning of the test when the rate was below 1 kHz. The analysis of the behavior in time showed that the initial slow increase of the background rate with time is explained by formation of new spots close to original 'bad' spot at

copper pins. Interestingly, the growth of new background spots is opposite to the direction of the gas flow. Furthermore, the sudden increase of the rate at the very end of the test is localized at the gas inlet of the counter, where no background discharges were existent in the beginning (Fig.13b).

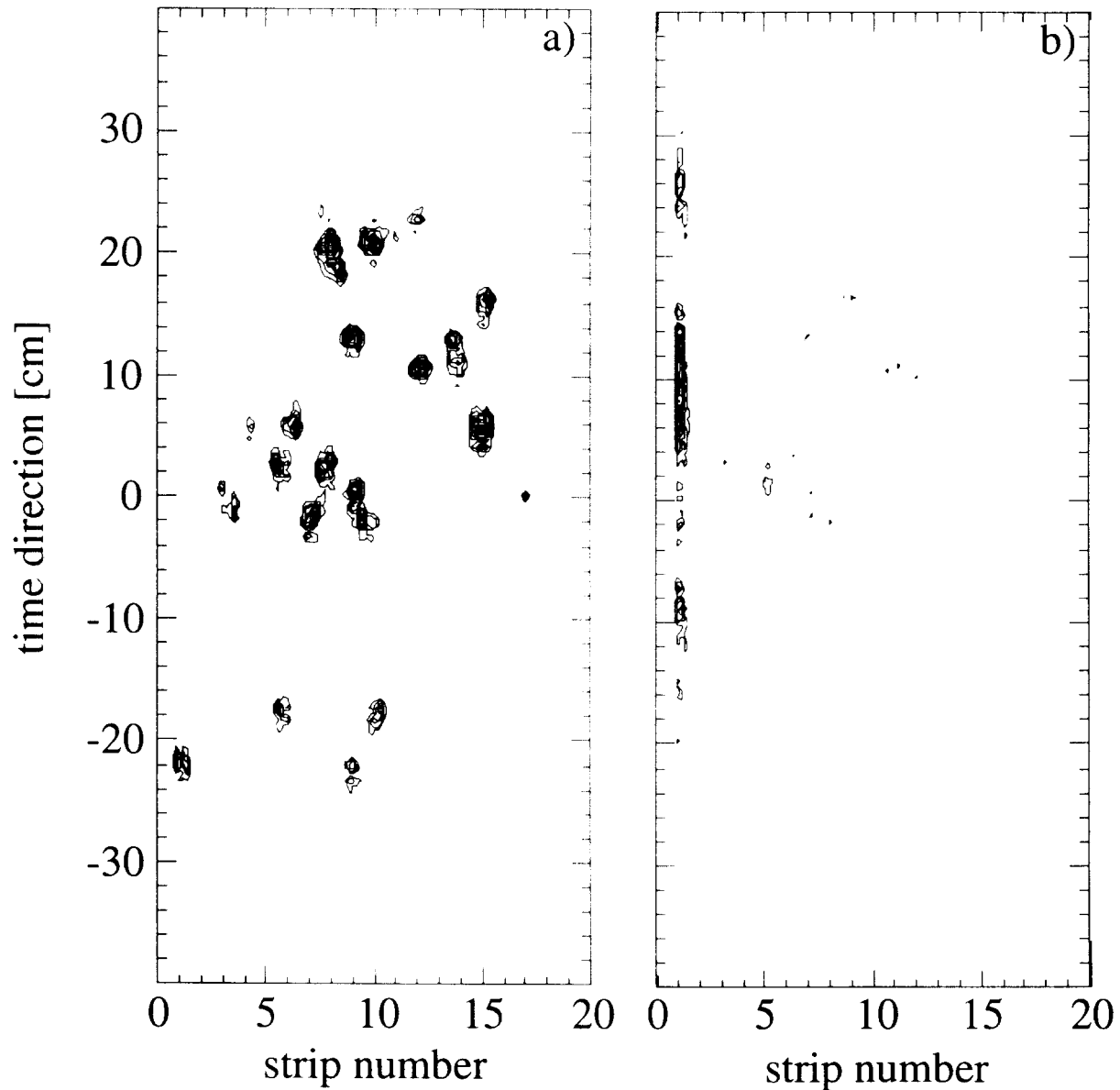


Fig. 13 Two-dimensional position distribution of hits in the counter. a) initial distribution at the beginning of the test; b) final distribution at the end of the test

A possible physical explanation of these results is a too high gas flow in the gap between the electrodes which causes turbulences in the counter. Turbulences appeared at the counter gas inlet because the cross section of the gas channel has sharp edges and also at 'bad' points due to collision of the gas flow and the shock waves from discharges.

Only a small fraction of the active counter area in this test was covered by background spots. In regions without 'bad' spots (>90% of the counter area) the rate remains at a very low level of about 0.05 Hz/cm<sup>2</sup> during the whole test (Fig. 12)

#### IV. Conclusions

In a beam test at CERN the performance of counter in terms of position and time resolution and efficiency reproduced the figures obtained at earlier test at Novosibirsk [2-7]. A 16-strip geometry, - suitable for the ALICE-LHC experiment-, was introduced and tested successfully.

After about one week of operation during which the voltage was raised from 3 to 4.4 kV background discharges appeared at the gas inlet. The subsequent long term stability test was performed at a 3 times reduced gas flow. The counter worked now stable during more than 3 months of operation, after which a similar behavior of background discharges at the gas inlet appeared. However, taken the higher operating voltage into account, this stands for a 50-70 fold improvement of lifetime. A further decrease of the gas flow in the counter as well an optimized shape of the inlet should stabilize the counter performance to the figures desired.

The exclusion of all 'bad' points on the counter electrodes from the very beginning is very important, because these act as "seed" for new background discharges. A different technology for the copper film deposition (sputtering) and rigorous quality control should solve this problem in the future.

#### V. Acknowledgement

We would like to thank Drs. B. Kolb and M. Purschke for their help in setting up the data acquisition at the CERN X1 test beam line and Dr. N. Kurz for his assistance during data taking at GSI

#### VI. References

- [1] Letter of Intent for ALICE, CERN/LHCC/93-16,LHCC/I 4 (1993)
- [2] Yu.N.Pestov, 4th San Miniato Topical Seminar, World Scientific (1991) 156
- [3] A.R. Frolov, Yu.N. Pestov and V.V. Primachek, Nucl.Inst. Meth. A307 (1991) 497
- [4] Yu.N. Pestov, Nucl. Inst. Meth. A265 (1988) 150
- [5] W.B. Atwood, G.B. Bowden, G.R. Bonneaud, D.E. Klem, A. Ogawa, Yu.N. Pestov, R. Pitthan and R. Sugaharal, Nucl. Inst. Meth. 206 (1983) 99
- [6] Yu.N. Pestov, Nucl. Inst. Meth 196 (1982) 45
- [7] V.V. Parkhomchuck, Yu.N. Pestov and N.V. Petrovykh, Nucl. Inst. Meth. 93 (1971) 269
- [8] Yu. Pestov, M.A. Tiunov, preprint BNIP 94-77 (1994), Ch. Neyer et al., GSI Ann. Report 94-1 (1994); Ch. Neyer et al., "A precise discriminator for Time-of-Flight measurements in ALICE", Proceedings of the first workshop on Electronics for LHC Experiments, Lisbon (1995)
- [9] A.R. Frolov, T.V. Osloпова, Yu. Pestov, , Nucl.. Inst. Meth. A356 (1994) 497
- [10] V.D. Laptev and Yu. Pestov, Pribyty i Tekhnika Eksperimenta, No. 6 (1975) 41